JCZ: Zoologischer Anzeiger - A Journal of Comparative Zoology 304 (2023) 94–104

Contents lists available at ScienceDirect

Zoologischer Anzeiger

journal homepage: www.elsevier.com/locate/jcz

Auditory system biophysics in a new species of false-leaf katydid (Tettigoniidae: Pseudophyllinae) supports a hypothesis of broadband ultrasound reception

Charlie Woodrow *, Fernando Montealegre-Z **

University of Lincoln, School of Life and Environmental Sciences, Joseph Banks Laboratories, Green Lane, Lincoln, LN6 7DL, UK

ARTICLE INFO

Handling Editor: Sven Bradler

Keywords:
Insect
Orthoptera
Taxonomy
South America
Bioacoustics

ABSTRACT

The auditory system of the katydid is an established model system for studies of hearing, predator-prey interactions, and cochlea dynamics. The components peripheral to the ear substantially influence the hearing threshold, with an internal auditory trachea tuned to the calling song of conspecifics, and external pinnae capable of enhancing ultrasounds for predator detection. The trade-off between such auditory pathways has been subject to multiple discussions, but received little experimental validation. In the most ultrasonic katydids (Pseudophyllinae and Meconematinae), it has been suggested that the external auditory pathway is of greater importance than the internal one, but the biophysical properties of the pinnae and tracheae in such groups have not been compared. Here, we describe the bioacoustics of a new species of pseudophylline katydid, *Eubliastes viridicorpus*. This species is found to produce a pure tone two-syllable song at 23.4 kHz, similar to other members of the genus. Using micro-CT scanning and finite element modelling, we describe the biophysical tuning of the internal auditory tracheae, and use 3D printed model experiments to investigate external auditory pinnae resonances. By modelling the natural resonant frequencies of the ear, we provide evidence that the acoustic trachea of *E. viridicorpus* female is tuned to the male song frequency. Experiments on 3D printed models of the pinnae demonstrate that *E. viridicorpus* has an external auditory pathway capable of broadband ultrasound amplification, providing pressure gains across an effective frequency range of 20–200 kHz, which could also provide enhanced reception of the male song. The importance of pinnae in ultrasonic rainforest katydids is discussed.

1. Introduction

The Pseudophyllinae (Orthoptera: Tettigoniidae), also known as the sylvan or false-leaf katydids, are a widespread orthopteran taxa within South American rainforest environments (Belwood, 1990; Montealegre-Z and Morris, 1999; Nickle, 1992), and have been present since at least the Middle Miocene (Song et al., 2015). Many species are characterised by their often large bodies and leaf-like wings, they are known for their diversity of forms of botanical mimicry; resembling the patterns and forms of leaves, wood, and even lichen, to avoid visual detection (Belwood, 1990).

This subfamily is well known for their unique acoustic and vibratory communication behaviours. They are among the most ultrasonic katydids, and while most species communicate in the low ultrasonic range (20–30 kHz), several genera are known to produce pure tone sounds exceeding 60 kHz (Mason et al., 1991; Morris et al., 1989; Stumpner et al., 2013; Suga, 1966). They also show low duty cycles in their acoustic signals (Belwood and Morris, 1987; Montealegre-Z and Morris, 1999; ter Hofstede et al., 2017), likely to reduce predation from eavesdropping predators, and tremulate in the absence of females, indicating that vibrations are a long-distance sexual signal which has replaced the need for loud or low frequency songs (Geipel et al., 2020; Morris et al., 1994).

The auditory system morphology of the Pseudophyllinae is also distinctive among the Tettigoniidae. Katydids possess paired tympanal ears in their forelegs, and sound can reach these tympana through two distinct pathways (Bailey, 1990). The primary route is via the acoustic trachea, or ear canal (Michelsen and Larsen, 1978; Nocke, 1975). This pathway is usually an exponential horn that runs through the forelegs with an opening, the acoustic (or prothoracic) spiracle, in the prothorax

* Corresponding author.
** Corresponding author.
E-mail addresses: cwoodrow@lincoln.ac.uk (C. Woodrow), fmontealegrez@lincoln.ac.uk (F. Montealegre-Z).

https://doi.org/10.1016/j.jcz.2023.04.002
Received 10 February 2023; Received in revised form 10 April 2023; Accepted 13 April 2023
Available online 14 April 2023

(Celiker et al., 2022; 2020; Hoffmann and Jatho, 1995; Jonsson et al., 2016; Nocke, 1975). Pseudophyllines have distinctly small acoustic spiracles, a taxonomic marker of the subfamily (Rentz, 1979), and these small spiracles are associated with uniquely narrow tracheae (Rajaraman et al., 2013). Small spiracles are not restricted to the Pseudophyllinae however, with some *Poecilimon* (Phaneropterinae) species (Stumpner and Heller, 1992), and female members of the Zaprochilinae (Bailey and Römer, 1991) showing similarly small openings to the auditory system.

As well as the internal auditory input, can reach the foretibial tympana externally, directly on the tympanum surface. Via this pathway, many katydids show auditory pinnae surrounding the tympana (Bailey, 1990; 1993; Pulver et al., 2022). The function of these pinnae has been hypothesised to range from protection and improved auditory directionality (Autrum, 1963; Bailey and Stephen, 1978; Schneider et al., 2017), to enhanced detection of ultrasonic predators (Pulver et al., 2022). The pinnae of the Pseudophyllinae are particularly large, open cavities (Bailey, 1990; Mason et al., 1991; Montealegre-Z and Robert, 2015; Rentz, 1979). Given these morphological properties, it has been hypothesised that members of this subfamily should show increased signal reception through the auditory pinnae rather than the trachea, particularly for high frequency ultrasounds (Mason et al., 1991; Pulver et al., 2022). These characteristics of the songs and ears of the Pseudophyllinae make this group an interesting model for studying many elements of predator-prey dynamics, insect signalling, and bioinspiration.

This study presents a new species of pseudophylline katydid of the tribe Cocconotini, and genus *Eubliastes* Beier, 1960, from a Pacific lowland rainforest in Colombia. The species is diagnosed using traditional morphological characters based on keys in the genus and related genera (Beier, 1962; 1960). In addition, we supplement this species description with information on acoustic ecology and auditory biophysics through lab-based calibrated sound recordings, μ-CT scanning, biophysical experimentation, and numerical simulation. We describe the male calling song and its relation to the resonances of the cavities surrounding the external tympanum using 3D printed models, and the *eigenfrequencies* (natural resonances) and *eigenmodes* (vibration patterns) of the acoustic tracheae. We hypothesised that the pinnae would have broadband resonances supporting the high frequency ecologies of this subfamily, and that the trachea would show resonances around the calling song frequency.

2. Methodology

2.1. Specimens

Sabaletas is located near the Anchicayá basin south of the city of Buenaventura in the Valle del Cauca, Colombia (3.741569 N, −76.967294 W). The collection site was a sheltered lodge located at 70 m elevation. Reaching the site is limited to access by boat leaving the town of Sabaletas. One adult male and one subadult female were collected after being found on the underside of the lodge shelter during a touristic diving trip.

2.2. Morphological measurements

We recorded the gross anatomy of *E. viridicorpus* using measurements with digital callipers (Fowler) and an Alicona InfiniteFocus microscope (Bruker Alicona Imaging, Graz, Austria) at 5x objective magnification. We collected images of the peripheral components of the auditory system, the tegmina and stridulatory file, and the terminalia. Using the built-in Alicona software, we then measured different anatomical features for comparisons to other members of the genus. Macro photos of the specimens were taken with a Nikon D7100 DSLR fitted with a Nikon NIKKOR AF-S 50 mm 1:1.8G lens (Nikon Inc., Tokyo, Japan) reverse mounted with a custom-built adapter and external flash (EF-610 DG Super, Sigma corporation, Japan). Digital illustrations of the male habitus and terminalia of both sexes were produced in Adobe Photoshop (Adobe Inc., San Jose, California).

2.3. Song recording

To record the species' acoustic signal under controlled conditions, we placed the male of *E. viridicorpus* in a mesh wire cage in an acoustic chamber (25 °C, 60% RH). The animal was provided food and water ad libitum. A B&K 1/8″ (3.2 mm) type 4138 omnidirectional microphone (Brüel & Kjær, Nærum, Denmark), calibrated using a B&K Type 4237 sound pressure calibrator (Brüel & Kjær, Nærum, Denmark) was positioned 10 cm from the wire cage. The microphone was set to record on trigger following sound production by the animal. The recording time was 16 s with 4 s prior to the trigger. Any successfully captured acoustic signals were recorded using a PSV-500 internal data acquisition board (PCI-4451; National Instruments, Austin, TX, USA) via a built in preamplifier (B&K 2670, Brüel & Kjær, Nærum, Denmark) and conditioning amplifier (Nexus 2690- OS1, Brüel & Kjær, Nærum, Denmark) at a sampling frequency of 512 kHz. A high-pass filter set at 1 kHz was used to remove any low frequency background noise, and final recordings were exported as.txt files for analysis. We analysed the song using MATLAB R2022a (MathWorks, Natick, USA) using the signal processing toolbox. The fundamental frequency, peak frequency, and bandwidth 20 dB below the peak frequency were extracted.

2.4. Auditory system anatomy and pinnae resonances

As part of a wider study on comparative auditory systems within the Ensifera, we μ-CT scanned the ears of deceased *E. viridicorpus* specimens using a SkyScan 1172 μ-CT scanner (12.9 μm voxel size, 55 kV source voltage, 200 μA source current, 200 ms exposure, 0.2° rotation step, Bruker Corporation, Billerica, MA, USA). μ-CT projection images were reconstructed to produce orthogonal slices with NRecon (v.1.6.9.18, Bruker Corporation, Billerica, MA, USA). For 3D segmentation, the slice data was imported into Amira-Aviso 6.7 (Thermo Fisher Scientific, Waltham, Massachusetts, USA) and the pinnae and tracheae selected using the magic wand tool every 5 slices throughout the whole ear, followed by interpolation to connect slices. The resulting materials were then used to generate a 3D surface and exported as an STL file (ascii format). At this stage, the cavities of the pinnae were filled as a separate material, and their absolute volume acquired using the material statistics tool in Amira-Aviso 6.7. Pinnae STLs were then 3D printed using a Mars Elegoo Pro 2 3D Printer (Elegoo Inc, Shenzhen, China). Models were printed using grey photopolymer resin (exposure parameters: 20 s first layer, 5 s normal layers) with a solidification wavelength of 405 nm. When printing was complete (about 1 h 30 min), models were washed in 100% isopropyl alcohol, rinsed in cold water, then exposed to UV light in an Elegoo Mercury Plus curing station (Elegoo Inc, Shenzhen, China) for 10 min 3D models were printed to be ~12 x larger than the real ear. Models were then stimulated with a loudspeaker with a calibrated B&K Type 4182 probe microphone (Brüel & Kjær, Nærum, Denmark) inside the anterior and posterior pinnae cavities (apc and ppc respectively) to record pinna cavity resonance. The microphone signal was amplified using a B&K 1708 conditioning amplifier (Brüel & Kjær, Nærum, Denmark). The effective tested frequency range of the stimulus after considering the scaling factor of the 3D print was 20–200 kHz, with all frequencies delivered at the same intensity (60 dB). This way, any resonances in the system would be identified as peaks in the frequency spectrum of the microphone response. For full details of the validated methodology, see Pulver et al. (2022). As well as biophysical experimentation, the theoretical resonances of pinnae were calculated following existing protocols (Pulver et al., 2022) to be compared to existing studies of pinnae resonance in other katydids. The same methods as above were also conducted on specimens of other members of the genus *Eubliastes* (*E. aethiops*, N = 2; *E. apolinari,* N = 1) that were

collected by FMZ on previous fieldwork trips.

2.5. Tracheae resonances

As well as description and biophysical measurement of the auditory pinnae, we conducted numerical models of acoustic trachea resonances. To investigate the natural frequencies and modes of resonance (*eigenfrequencies* and *eigenmodes*) of the tracheae, STLs from μ-CT scanning were imported into COMSOL (v5.6, COMSOL Multiphysics, Burlington, MA), and a 3D mesh generated. Where mesh generation failed on the first attempt, the STL was imported into Netfabb (Netfabb 2022; Autodesk Inc., Lupburg) for default STL repair, and then re-imported into COMSOL. STLs were imported with default simplification tolerance. After successful mesh generation, the material inside the trachea was selected to be air and given the properties of air under default temperature settings (293.15 K). Edges for the acoustic spiracle and two tympana were defined manually within the mesh using the 'create entities' function. The acoustic spiracle, tympana, and trachea wall could then be assigned unique boundary properties. The acoustic spiracle was given a boundary of plane wave radiation; a class of non-reflecting boundary conditions which permits the passage of a plane wave without resistance, which accurately reflects ports such as the opening to a tube where the medium inside and outside the tube are the same (COMSOL Multiphysics, v5.6 Reference Manual, 2018).

The acoustic trachea wall was assigned as a hard sound boundary, where the normal component of acceleration is zero, using following the formulation:

$$-n \bullet \left(-\frac{1}{\rho_0}(\nabla p - q) \right) = 0 \qquad \text{Eq. 1}$$

Where ρ = density (kg m-3), p = pressure (Pa), q = dipole source of displacement (N m-3). The two tympana were assigned as boundaries with an acoustic impedance, where part of the wave is transmitted across and part is reflected, dependant on the impedance, following the formulation:

$$-n \bullet \left(-\frac{1}{\rho_0}(\nabla p - q) \right) - \frac{i\omega p}{Z} = 0 \qquad \text{Eq. 2}$$

Where i = $\sqrt{}$-1, ω = angular frequency (rads/s), and Z = acoustic impedance (Pa * s/m). Z was chosen to be a 1000 Pa * s/m across all models, reflecting the average known impedance value for the tympana of the katydid *Copiphora gorgonensis* (Celiker et al., 2020). *Eigenvalues* were solved using the ARPACK *eigenfrequency* solver, with a linear elastic pressure model (stress: strain = 1: 1). The *eigenfrequency* solver follows the formulation:

$$\nabla \bullet \left(-\frac{1}{\rho_c}\nabla \mathrm{p} \right) + \frac{\lambda^2 p}{\rho_c C^2} = 0 \qquad \text{Eq. 3}$$

Where C = speed of sound in the medium (m s-1) and λ = *eigenvalue*. The subscript 'c' denotes that the variable ρ can be a complex number. The *eigenvalue* lambda is related to the calculated *eigenfrequency* (f) and angular frequency (ω) using:

$$\lambda = i2\pi f = i\omega \qquad \text{Eq. 4}$$

The sound pressure was assumed to be 1 Pa, and the velocity 343 m/s. The first 4 natural frequencies of the trachea were solved, and images of the *eigenmodes* at each of these *eigenfrequencies* exported as JPEGs.

3. Results

3.1. Taxonomy

Order ORTHOPTERA Olivier, 1789
Superfamily TETTIGONIOIDEA Krauss, 1902
Family TETTIGONIIDAE Krauss, 1902
Subfamily group PHANEROPTERIDAE Burmeister, 1838
Subfamily PSEUDOPHYLLINAE Burmeister, 1838
Supertribe Pleminiiti Brunner von Wattenwyl, 1895
Tribe Cocconotini Brunner von Wattenwyl, 1895
Genus Eubliastes Beier, 1960.
Type species. — *Eubliastes (*synonym: *Cocconotus) adustus* (Bolívar, 1881).
Eubliastes viridicorpus sp. nov.

Material examined. - **Holotype:** COLOMBIA • ♂; Sabaletas, Buenaventura, Valle del Cauca, Colombia; (3.741569 N, −76.967294 W); F Montealegre-Z; IAVH. **Allotype:** COLOMBIA • ♀; Sabaletas, Buenaventura, Valle del Cauca, Colombia; (3.741569 N, −76.967294 W); F Montealegre-Z; IAVH; captured as subadult juvenile, attempt to rear to adult in captivity successful but fall during final molt resulted in loss of hindlegs and damage to ovipositor (folded in half laterally, but recoverable for identification and suitable illustrated reconstruction) and wings (completely damaged). Head, thorax, and forelegs not damaged by failed molt.

Type locality. - Sabaletas, Buenaventura, Valle del Cauca, Colombia.

Etymology. - Meaning 'green body' named after the bright colours which differentiate the species from other *Eubliastes* spp.

Diagnosis. – *E. viridicorpus* is placed within the genus *Eubliastes* due to darkened dorsal surface of head and pronotum; long elytra with yellow venation; gradually compressed pronotum with anterior granulation and thick lateral margins. There are nine other valid species in the genus *Eubliastes* (Cigliano et al., 2023). In *E. viridicorpus*, there is a distinct U-shaped marking at the base of the frons, the corners of which point to the base of the eyes, and two dots centrally. The dorsal margin of the frons has further markings which are continuous from left to right eye. Other features of *E. viridicorpus* which diagnose it from the other nine species include the unique globular shape of the male cerci, which display a single spine on the inner ventral edge rather than the cercal tip, and the sharp angle between the male subgenital plate and the elongate styli (For measurements, see Table 1).

Description. – Head: around 1.4x longer than wide, with eyes that do not extend far beyond the gena laterally. Postclypeus (dorsal clypeus) black. Dorsal frons and gena black. Frons with distinct U-shaped marking ventrally and two dots centrally (Fig. 1A and B).

Thorax: Mostly vivid green in colour, with beige/amber moving ventrally, and black markings on dorsal margins of all leg coxae

Table 1
Body measurements of *Eubliastes viridicorpus sp. nov.* All measurements in mm. For paired features (e.g. legs) left/right features reported respectively. n.a. = not applicable, where the structure was not present to be measured (e.g. damaged, absent, or not present due to sex differences).

Parameter	♂ (N = 1)	♀ (N = 1)
Body length	37.50	38.50
Tegmen length	40.10/40.20	39.56/n.a.
Pronotum length	10.39	11.10
Pronotum width	8.35	9.55
Fore-femur length	16.88/n.a.	17.23/17.20
Fore-tibia length	17.5/n.a.	19.14/19.13
Mid-femur length	16.94/16.93	18.24/n.a.
Mid-tibia length	19.20/19.15	20.05/n.a.
Hind-femur length	38.4/38.5	n.a.
Hind-tibia length	39.7/39.8	n.a.
Head width	6.72	7.64
Head length	10.09	10.79
Cercus length	3.83/3.84	4.16/4.19
Subgenital plate length	4.66	3.38
Subgenital plate width (at base)	3.12	4.85
Styli length	3.04/3.06	n.a.
Ovipositor length	n.a.	21.5
Ovipositor height (at base)	n.a.	4.87
Stridulatory file length	3.60	n.a.

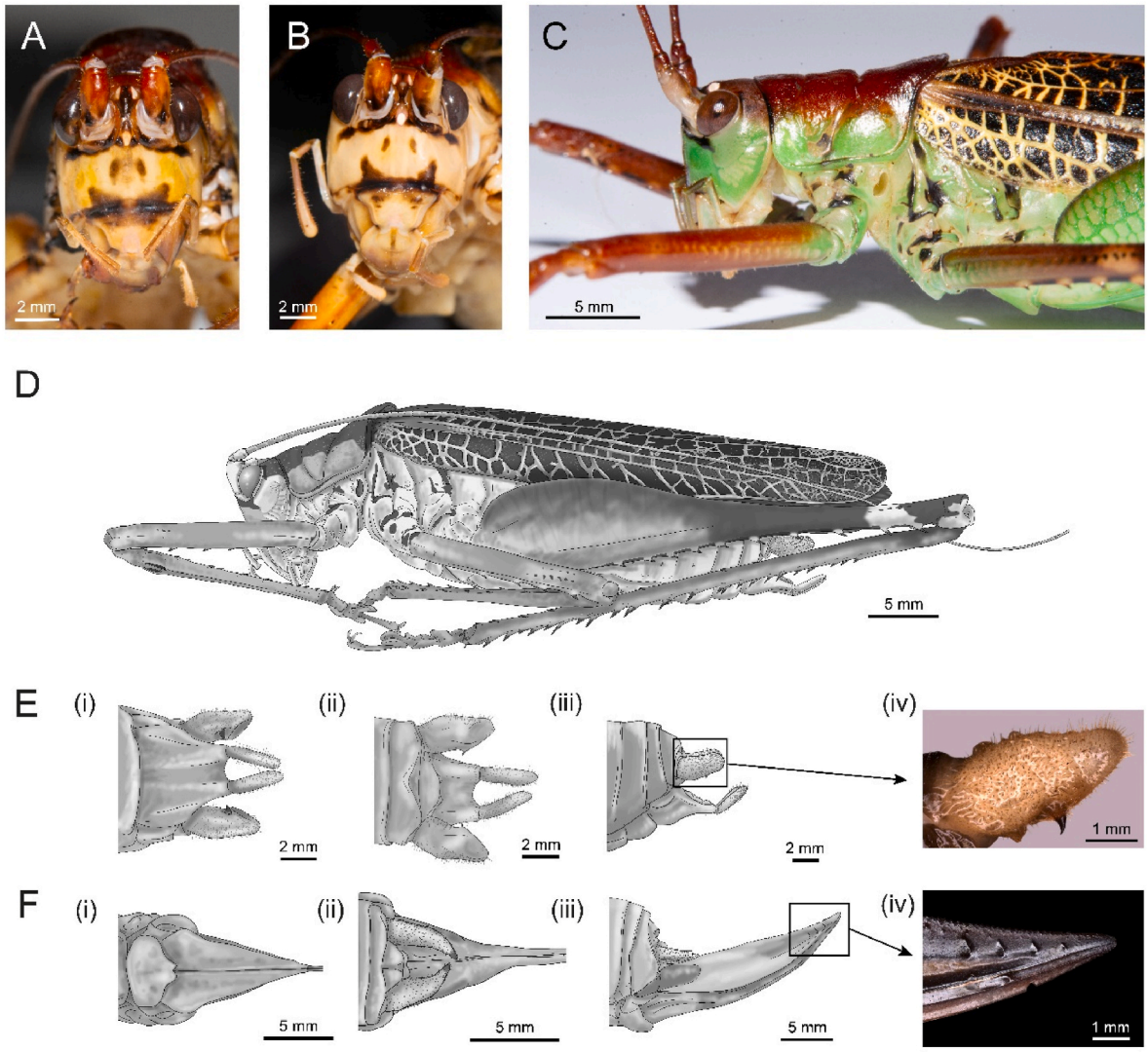

Fig. 1. *Eubliastes viridicorpus sp. nov.* A. male face; B. female face; C, male alive; D. illustrated male habitus; E, illustrated male terminalia in ventral (i), dorsal (ii), and lateral (iii) views with lateral view of left cercus (iv); F, female terminalia in ventral (i), dorsal (ii), and lateral (iii) views with lateral close up of ovipositor tip (iv). Note, colours of the face in A and B are an artifact of alcohol preservation, but markings remain accurate. Illustrations by CW.

(Fig. 1C). The acoustic spiracle in the prothorax is small as expected for the subfamily, and kidney bean shaped (Fig. 1C).

Legs: Forelegs and midlegs dorsally unarmed, ventrally with four pairs of spines on tibiae. Foretibae bearing large tympanal organ with wide pinnae, and eight pairs of ventral spines, with first pair distal of the tympanal organ. All legs reddish-brown with vivid green towards coxae. Midfemur and hindfemur with light beige/amber band towards distal end before joint. Beige/amber band contains dark spots, 5–7 in sequence on all femurs. Mid- and hindfemur spines light beige/amber at base, black at tip. Hindfemur armed with ten ventral spines. Hindtibiae armed with 12 pairs of spines ventrally and 17 dorsally. Genicular lobes rounded and without dark pigmentation.

Wings: Large, extending distally beyond terminalia but not beyond hindlegs (Fig. 1D). Striking yellow venation pattern. Within-cell tegminal colour black rather than the vivid light green of *E. chlorodictyon* (Montealegre-Z and Morris, 1999), or the ochraceous tawny brown of other members of the genus (Fig. 1C). Male stridulatory field large and circular, with strongly raised CuPb vein and stridulatory file. Stridulatory file with 262 teeth. Wings shorter than *E. pollonerae* (Beier, 1960).

Abdomen: Follows colour pattern of thorax, with mostly vivid green colour dorsally, with beige/amber moving ventrally. Lacks black markings as seen on thorax.

Terminalia: Male: subgenital plate elongate without strong emargination, centrally depressed (Fig. 1E(i)), with two long styli. 10th tergite truncate with central emargination (Fig. 1E(ii). Cerci large, beige/white, and robust, with curved spine on inner edge (Fig. 1E(iii)). Styli at unique obtuse angle with subgenital plate (Fig. 1E(iii)). Female: subgenital plate isosceles triangular with rounded subbasal lobes and pronounced soft V-shaped emargination (Fig. 1F(i)). Cerci cream white, pointed with spine (Fig. 1F(ii)). Ovipositor broad, smooth with distal serrations dorsally, and four lateral notches; reddish-brown and basally amber/beige (Fig. 1F(iii)).

Coloration. – In live animal colours unusually bright for genus (Fig. 1C). Dorsal pronotum and head a cordovan brown colour, with a lateral gradient typical of the genus. Ventral edges of pronotum, head, and most of body a vibrant green. Frons a deeper vibrant green. Wing venation electric yellow. Within-cell tegminal colour black. Large male cerci and distal patch on hind femur matching in light beige. Bases of spines on hind femur also beige. Markings on face and legs black.

Comments. – In Beier's key to the genus and more recent descriptions, this species has dorsally unarmed middle tibiae, and the anal margins of the tegmina are not darkened, placing it closely with *E. chlorodictyon*. The next character choice is based on the pronotum, which will either have black, reddish-brown, or light amber lateral lobes. *E. viridicorpus*

does not fit any of these descriptions, with vivid green lateral pronotal lobes (Fig. 1C). *E. viridicorpus* is most similar in overall morphology to *E. chlorodictyon* (Montealegre-Z and Morris, 1999), but displays distinct features which we have used to distinguish *E. viridicorpus* as a new species. Frons of *E. viridicorpus* displays additional markings absent in *E. chlorodictyon*. *E. viridicorpus larger* than *E. chlorodictyon*, with eyes smaller relative to the head width. Face markings distinct from *E. aethiops*, which has two marks extending down from the eyes, and three markings on the ventral frons. Male subgenital plate much shorter than *E. chlorodictyon*, lacking the V-shaped emargination, with longer styli than *E. chlorodictyon.* Sharp angle between the male subgenital plate and the elongate styli in *E. viridicorpus* is similar to *E. adustus* but styli much shorter. Male cerci substantially more robust in *E. viridicorpus* than any other members of the genus, with spine located on inner edge rather than cercal tip. Male subgenital plate and styli similar to *E. festae* but cerci more elongate in *E. festae* than *E. viridicorpus*, with larger final abdominal tergite in *E. festae*. Female ovipositor much larger and broader in both *E. ferrugineus* and *E. pollonerae* than *E. viridicorpus.* Ovipositor less elongate in *E. viridicorpus* than *E. conspersus.* Female ovipositor is instead most similar to *E. apolinari*, but with four short oblique ridges rather than five. Female subgenital plate smaller and less ventrally protruding than *E. ferrugineus* and *E. pollonerae.*

3.2. Sound production and stridulatory apparatus

The song of *Eubliastes viridicorpus* sp. *nov.* was recorded in a controlled laboratory environment within a sound-proof booth. This species exhibits a transient singing behaviour. The duration of the song is ~0.1 s, consisting of two syllables (Fig. 2D) representing two closing strikes of the stridulatory apparatus. The song duty cycle is low, with silence for several minutes before the two syllables are repeated. The song had a highest recorded amplitude of 1.36 Pa or ~96.7 dB SPL (re. 20 μPa at 10 cm) at a peak frequency of 23.4 kHz (Fig. 2D). At −20 dB below this peak, the spectral breadth ranged from 21.9 to 24.1 kHz. The signal also displays a strong peak at 11.7 kHz, which can be referred to as the fundamental frequency of the song. At −20 dB below this peak, the spectral breadth ranged from 10.9 to 12.5 kHz (Fig. 2E). The waveform shown in the inset in Fig. 2E reflects the harmonic interaction observed in the frequency analysis.

3.3. Auditory system anatomy and pinnae resonances

Three key parts of the auditory system of *Eubliastes viridicorpus* sp. *nov.* were imaged to accompany the species description (Fig. 3A and B). The internal input to the auditory system, the acoustic spiracle, was small as typical of the Pseudophyllinae, averaging an area of 0.56 mm^2 in the male, and 0.59 mm^2 in the female. This spiracle opens to an acoustic trachea with a length and volume of 40.33 mm and 8.47 mm^3 respectively in the male, and 41.45 mm and 9.10 mm^3 respectively in the female. The external input to the auditory system, the tympanal pinnae, are symmetrical, with a mean pinnal slit area of 0.32 ± 0.01 mm^2 in the male and 0.36 ± 0.01 mm^2 in the female. The mean volumes of the anterior pinnae cavities (apc) and posterior pinnae cavities (ppc) were 0.40 ± 0.05 mm^3 in the male and 0.41 ± 0.04 mm^3 in the female. These auditory pinnae were 3D printed and simulated with real sound, with stimulus wavelengths scaled to consider the size of the 3D models compared to the real ears (Pulver et al., 2022). Experimental measurements of the 3D printed models revealed peak resonances averaging 71.16 kHz for the male pinnae, and 72.95 kHz for the female pinnae (Fig. 3C–D), although the overall pinna response was broad, providing a pressure gain of >3 dB SPL for all tested frequencies (20–200 kHz). These experimental and morphological measurements were repeated in specimens of *E. aethiops* and *E. apolinari* for comparisons across the genus (Table 2). In *E. aethiops*, peak pinna resonances averaged 89.2 kHz

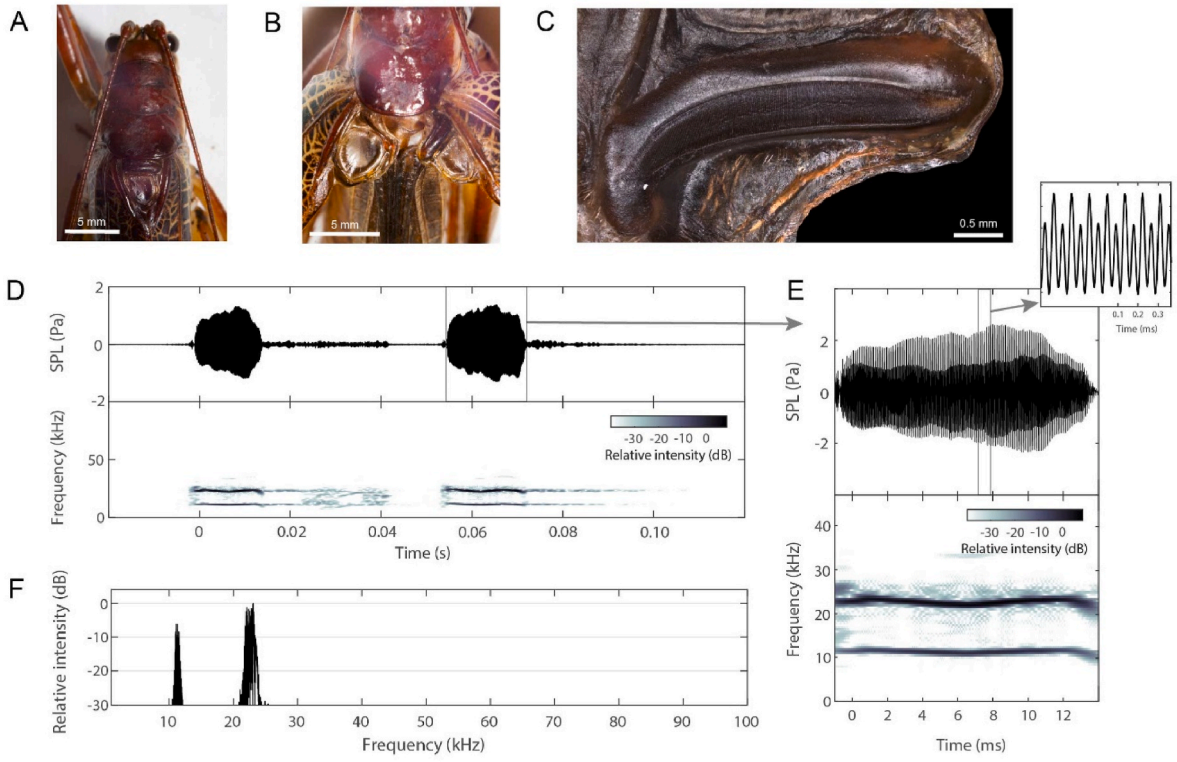

Fig. 2. *Eubliastes viridicorpus sp. nov.* acoustics. A, dorsal view of male stridulatory apparatus with tegmina closed; B, dorsal view of male stridulatory apparatus with tegmina open; C, male stridulatory file; D, male calling song waveform and spectrogram; E, waveform and spectrogram of single pulse, with high resolution inset of the dual tone waveform; F, male calling song frequency spectrum. Spectrogram parameters: FFT size = 512; Hamming window = 50% overlap; frequency resolution = 500 Hz.

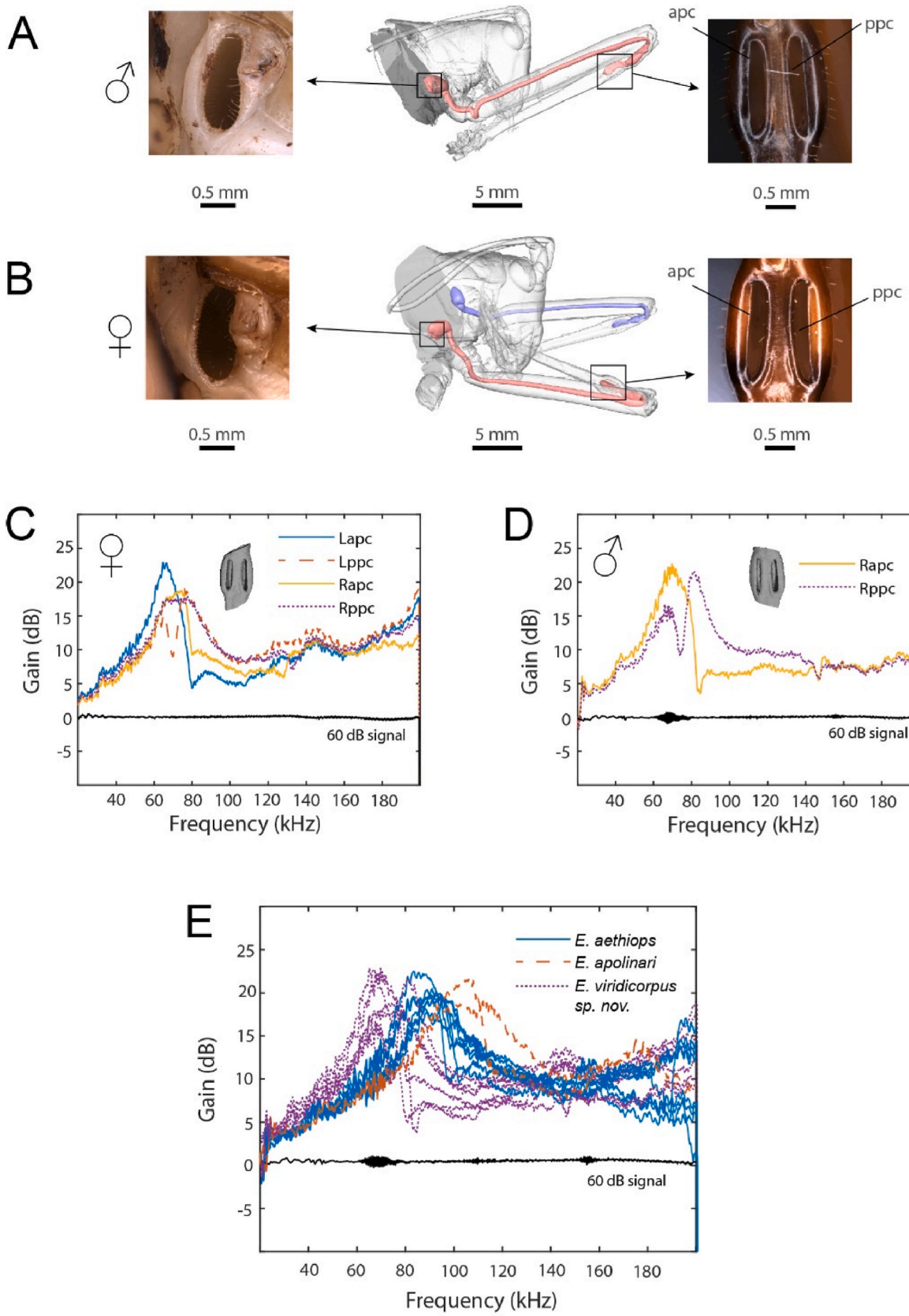

Fig. 3. *Eubliastes viridicorpus sp. nov.* auditory system. A. male auditory system: (left to right) acoustic spiracle, acoustic trachea, auditory pinnae; B. female auditory system (left to right same as A); C. female auditory pinnae resonances; D. male auditory pinnae resonances; E, auditory pinnae resonances across other species of the genus *Eubliastes*. Abbreviations: Lapc, Left anterior pinna cavity; Rapc, Right anterior pinna cavity; Lppc, Left posterior pinna cavity; Rppc, Right posterior pinna cavity.

Table 2
Auditory system anatomy measurements. All measurements are averaged across left and right side of the body. For each, N = 1.

Parameter	*Eubliastes viridicorpus* sp. *nov.* ♂	*Eubliastes viridicorpus* sp. *nov.* ♀	*Eubliastes aethiops* ♂	*Eubliastes aethiops* ♀	*Eubliastes apolinari* ♂
Acoustic spiracle area (mm^2)	0.56	0.59	0.34	0.31	0.19
Acoustic trachea length (mm)	40.33	41.45	28.18	26.24	22.09
Acoustic trachea volume (mm^3)	8.47	9.10	4.01	4.30	2.51
Auditory pinna anterior slit area (mm^2)	0.31	0.35	0.21	0.24	0.15
Auditory pinna posterior slit area (mm^2)	0.33	0.37	0.23	0.25	0.17
Auditory pinna anterior cavity (apc) volume (mm^3)	0.43	0.43	0.19	0.20	0.11
Auditory pinna posterior cavity (ppc) volume (mm^3)	0.36	0.38	0.20	0.20	0.11
Anterior pinna neckless-Helmholtz resonance (kHz)	66.93	62.3	76.5	82.6	84.8
Posterior pinna neckless-Helmholtz resonance (kHz)	71.42	69.9	79.2	84.4	91.0

in the female specimen and 94.9 kHz in the male specimen, while the single male specimen of *E. apolinari* had average peak pinna resonances of 109.12 kHz (Fig. 3E). Experimental measurements of pinnae resonance were similar to values predicted from an equation for neckless Helmholtz resonance (Table 2). The experimental resonances were consistently higher than the values predicted by this equation, likely due to the equation assuming a circular opening and spherical cavity.

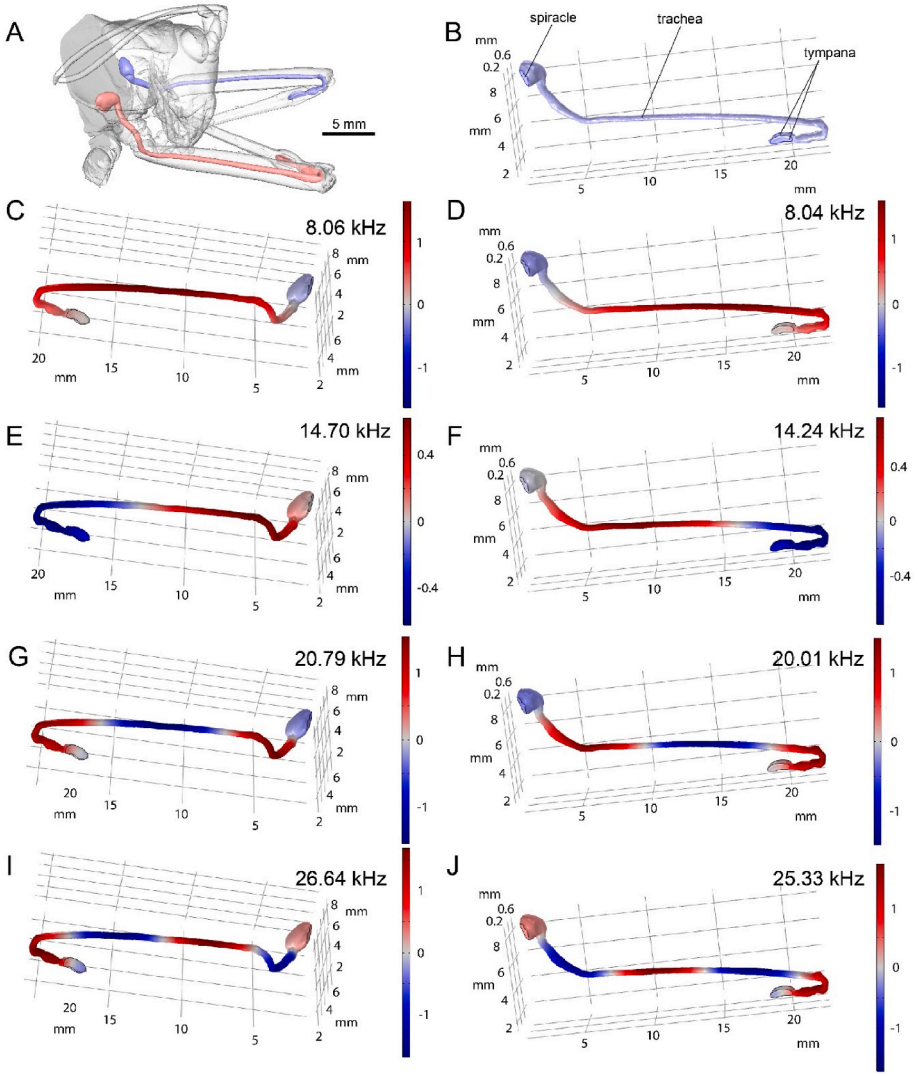

Fig. 4. *Eubliastes viridicorpus sp. nov.* female tracheae resonances. A, female acoustic tracheae; B, right trachea anatomy showing model boundary conditions; C, left trachea first *eigenfrequency*; D, right trachea first *eigenfrequency*; E, left trachea second *eigenfrequency*; F, right trachea second *eigenfrequency*; G, left trachea third *eigenfrequency*; H, right trachea third *eigenfrequency*; I, left trachea fourth *eigenfrequency*; J, right trachea fourth *eigenfrequency*.

3.4. Tracheae resonances

To compare passive elements of auditory tuning, an *eigenfrequency* analysis was conducted in COMSOL. The natural frequencies of the system were modelled for the adult female tracheae, to investigate tuning to the male song. The first four *eigenfrequencies* and *eigenmodes* of the tracheae were reported (Fig. 4). The trachea has natural resonances around 8, 14, 20, and 26 kHz.

4. Discussion

4.1. Taxonomy

The tribe Cocconotini is a rich katydid taxon, with 36 valid genera representing 143 species (Cigliano et al., 2023). The genus *Eubliastes* is the third most speciose genus within this tribe, with nine species. *Eubliastes viridicorpus* is described as a new species to science and the tenth member of the genus *Eubliastes* based on morphological evidence, and through comparisons to the acoustic signals of other members of the genus. The most obvious characteristic traits of *E. viridicorpus* are its green colouration, which is unusual for the genus, and the male terminalia, which are uniquely robust. The species is not placed within a new genus based on the unusual colour and male terminalia due to other similarities with existing *Eubliastes* spp.

4.2. Acoustics of Eubliastes spp.

The song of *E. viridicorpus* is classic for members of the Cocconotini, showing discrete pure tone pulses with a similar envelope structure to other pseudophyllines (Baker et al., 2019; Stumpner et al., 2013) peaks at 23.4 kHz and is most similar to that of *E. aethiops*, which is also comprised of two syllables at a similar peak frequency (23.9 kHz, Fig. A1). However in *E. aethiops* the frequency spectrum has a wider bandwidth of 11.9 kHz (20 dB below the peak) compared to 2.2 kHz in *E. viridicorpus*, and does not show the additional frequency component towards 12 kHz as seen in *E. viridicorpus*. This song peak frequency range seems to be characteristic of the genus with *E. chlorodictyon* and *E. pollonerae* singing at and 25.4 and 25.5 kHz respectively (Figs. A2,A3; Montealegre-Z and Morris, 1999; ter Hofstede et al., 2020).The same could be said of the two syllable temporal pattern of the song, but more recordings of other extant species (acoustic data is currently only available for four species) would be beneficial for future comparisons. The song of *E. viridicorpus* is also interesting in that the high amplitude component is at the start of each syllable rather than the end. This is similar to the song structure of *E. chlorodictyon* (Montealegre-Z and Morris, 1999), but differs from *E. aethiops* (Fig. A1) and *E. pollonerae* (ter Hofstede et al., 2020). This difference is not due to differences in stridulatory file anatomy, but instead indicates that the pattern of wing motion during stridulation differs, as the loudest component of the signal is produced during wing closure (Montealegre-Z., 2005; Montealegre-Z et al., 2006; Nielsen and Dreisig, 1970). Although tremulation was observed in the field, we were not able to record tremulatory signals in the laboratory. We hypothesise that *E. viridicorpus* utilises wing velocity to generate the lower peak of the song spectrum, but with a mirror tuned to the higher frequency peak of the spectrum (the first order harmonic) to optimise energy use.

4.3. Auditory system biophysics

Using 3D printed models and numerical simulations, the biophysical tuning of the pinnae and acoustic tracheae were measured. The pinnae amplified ultrasonic frequencies by up to 23 dB, supporting existing studies on the role of pinnae in high frequency reception (Pulver et al., 2022). However the pinnae of *E. viridicorpus* show a much broader response to those in Pulver et al. (2022), amplifying all sounds across the tested frequency range, including the frequency of the male song by up to 5 dB. The same was observed for *E. aethiops* and *E. apolinari*, where peak pinnae resonances differed but the overall response was also broadband amplification. This supports previous hypotheses of the pinnae as the dominant auditory input in the Pseudophyllinae (Mason et al., 1991), and supports the implication that the acoustic trachea may have a reduced function. Despite this, the trachea may still be used for conspecific detection, as numerical models revealed the female trachea has natural resonances ~25 kHz, which could function for amplification of the male song. In addition, the pinnae experiments do not consider the air in the tympanic cavities, but are static models of the sub-slit cavities, thus real pinnae resonances may differ through coupling of the tracheal branches beneath the tympanum. If both the pinnae and the tracheae are able to function as auditory inputs around the calling song frequency, we may infer that the pressure-difference receiver function of the ear provides strong directional cues, but these cues would then vary with leg position, making further neuronal processing challenging (Jonsson et al., 2016; Michelsen and Larsen, 2008). For higher frequencies, where the trachea is likely to provide a sound pressure loss (Celiker et al., 2020), the ears are more likely to function as simple pressure receivers. This could be an interesting hypothesis to investigate in the context of how these katydids localise their echolocating predators, as localisation without a pressure-difference receiver requires central processing of stimulus time and amplitude between the ears rather than a comparison of phase difference (Michelsen, 1979). In this case, neuronal sharpening of binaural cues may not be necessary, and contralateral inhibition may serve a more important function (Reeve and Webb, 2003).

The differences in pinna anatomy and function between the Pseudophyllinae presented here and the cone-headed katydids (Conocephalinae) demonstrated in Pulver et al. (2022) are clear. Pseudophyllines have larger pinna slits (average 0.26 mm^2 across the presented *Eubliastes* species and average 0.16 mm^2 in *Copiphora gorgonensis*), and larger pinna cavity volumes (average 0.26 mm^3 across the presented *Eubliastes* species and average 0.145 mm^3 in *C. gorgonensis*). These differences in geometry result in differences in resonance, with the smaller pinnae of *C. gorgonensis* having higher frequency peak resonances (Pulver et al., 2022). However, we should be careful to categorise pinnae based on their peak resonances, as the responses across both taxa are broad, with *C. gorgonensis* amplifying all sounds from ~55 to 150 kHz, and *Eubliastes* species amplifying all sounds from ~20 to 200 kHz. While pinnae function may be for enhanced ultrasound detection (Pulver et al., 2022), the precise peak frequency of this amplification is probably irrelevant, as katydids are popular prey species of predators utilising a range of ultrasounds for foraging (Römer and Holderied, 2020; Schulze and Schul, 2001; ter Hofstede et al., 2017; Zou et al., 2022), whereby natural selection will favour ears which act as wide-spectrum receivers (Bailey and Stephen, 1978).

Furthermore, small sample sizes in this study limit our understanding of within-species variation in auditory system anatomy and function. Future behavioural and biophysical experiments on further pseudophylline katydids in the lab and field would be beneficial.

4.4. Pinnae in the Pseudophyllinae and Meconematinae

It would be sensible to predict, based on these findings, that pseudophyllines which communicate at frequencies beyond the function provided by the acoustic trachea (<60 kHz; Celiker et al., 2020) may have lost function of the trachea, switching instead to utilising the high amplitude gains of the external auditory pinnae (Pulver et al., 2022) for conspecific sound reception (Mason et al., 1991). Morphological data we are collecting as a wider study of katydid auditory systems supports this hypothesis (Woodrow, unpublished). This is likely to also be the case in the extreme ultrasonic Meconematinae (*Supersonus* and *Arachnoscelis* spp.), where calling song frequencies range from ~70 kHz over 150 kHz. Wider comparative studies of auditory trachea and pinnae function, combined with numerical simulation and biophysical experimentation, are in process to develop this hypothesis.

Funding

CW's PhD studentship is funded by the University of Lincoln's School of Life and Environmental Sciences. This study was funded by a European Research Council Grant ERCCoG-2017-773067 (to FMZ for the project "The Insect Cochlea") and an NSF - NERC grant NSF DEB-1937815 - NE/T014806/1 (to FMZ).

Author contributions

CW conducted micro-CT scans, 3D printing, data collection and analysis, and writing. FMZ conducted song recording, specimen collection, permits, supervised, and oversaw the study.

Declaration of competing interest

The authors declare the following financial interests/personal relationships which may be considered as potential competing interests: Fernando Montealegre-Z reports financial support was provided by European Research Council. Fernando Montealegre-Z reports financial support was provided by Natural Environment Research Council. Charlie Woodrow reports financial support was provided by Orthopterists' Society.

Data availability

Data will be made available on request.

Acknowledgements

We thank the Orthopterist's' society for aiding in the funding of the μ-CT work of CW, for which data has been used in this study. We thank Thorin Jonsson, Fabio Sarria-S, Jorge Vargas Sarria, and Antonio "Toño" Asprilla for assistance during fieldwork. Specimens were collected under the research permit DTS0-G-090 granted by the Colombian Authority to FMZ. We thank two anonymous referees who significantly improved the manuscript.

Appendices.

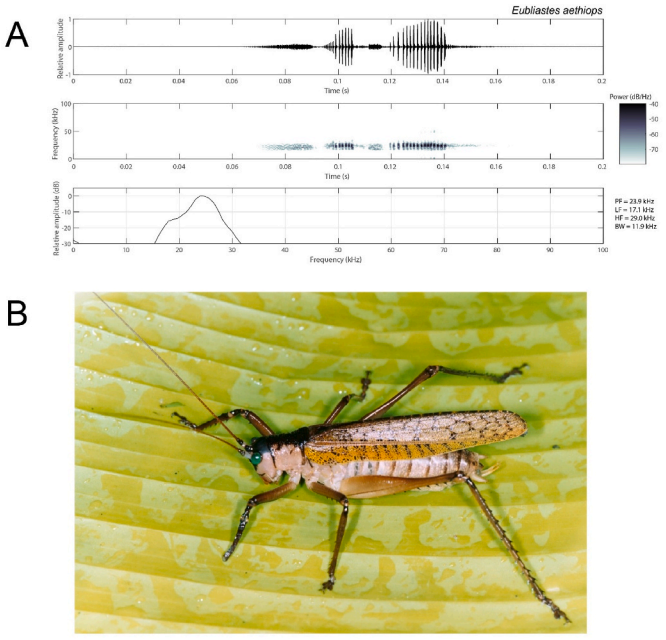

Fig. A1. Calling song of *Eubliastes aethiops* male. A, calling song, Top, waveform; middle, spectrogram; bottom, frequency power spectrum. PF = peak frequency; LF = low frequency (20 dB below PF); HF = high frequency (20 dB below PF); BW = bandwidth (HF-LF). B, male specimen in the field (photograph by Fernando Vargas-Salinas). Spectrogram parameters: FFT size = 512; Hamming window = 50% overlap; frequency resolution = 500 Hz

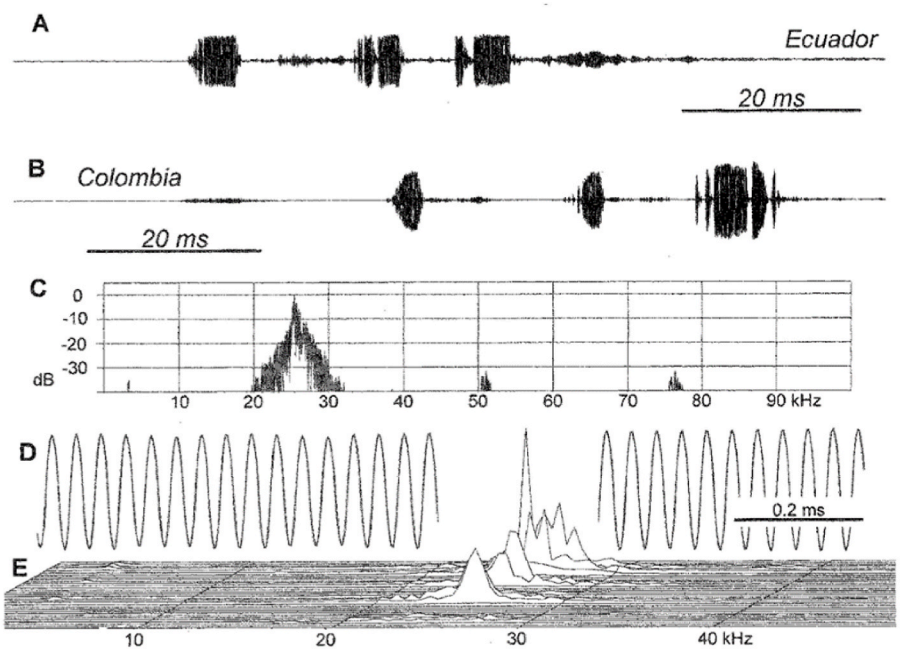

Fig. A2. Calling song of *Eubliastes chlorodictyon* from Montealegre-Z and Morris (1999). Caption: 'Ecuador specimen: A, Single call. Colombian specimen: B, Single call. C, Power spectrum. D, Portion of a pulse at high resolution showing sinusoid waveform. E, Waterfall spectral display of one call.

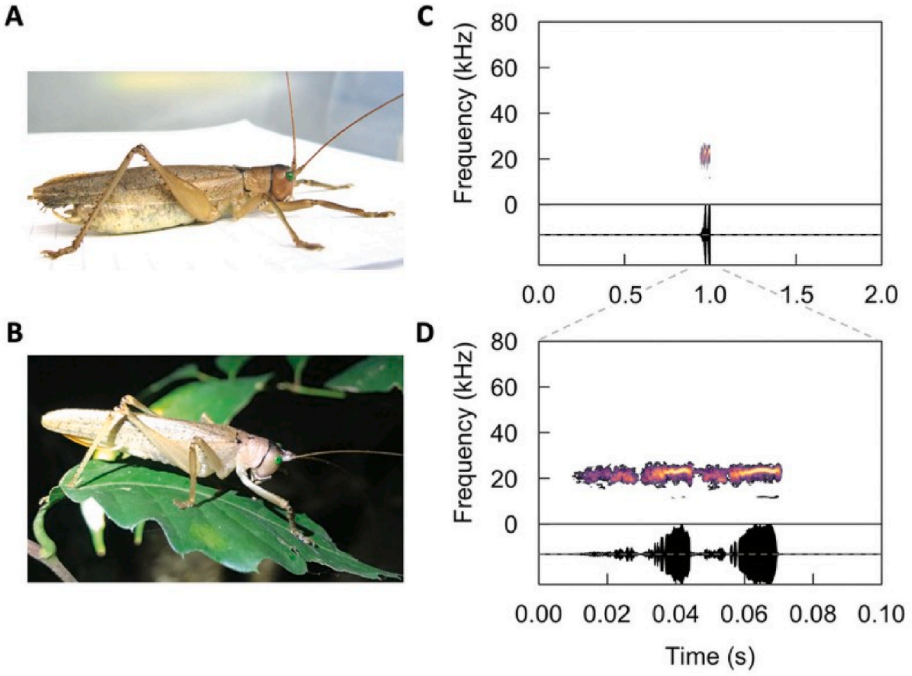

Fig. A3. Calling song of *Eubliastes pollonerae* from ter Hofstede et al. (2020). Caption: 'Photographs and calling song spectrograms of *Eubliastes pollonerae*. A. Male (photo credit: H. ter Hofstede); B. Female (photo credit: C. Kernan); C. and D. Spectrogram (top panel) and oscillogram (bottom panel) of one call at different time scales'.

References

Autrum, H., 1963. Anatomy and physiology of sound receptors in invertebrates. In: Busnel, R.G. (Ed.), Acoustic Behaviour of Animals. Elsevier, pp. 412–433.

Bailey, W.J., 1993. The tettigoniid (Orthoptera : tettigoniidae) ear: multiple functions and structural diversity. Int. J. Insect Morphol. Embryol. 22, 185–205. https://doi.org/10.1016/0020-7322(93)90009-.

Bailey, W.J., 1990. The ear of the bushcricket. In: Bailey, W.J., Rentz, D.F.C. (Eds.), The Tettigoniidae: Biology, Systematics and Evolution. Springer Berlin Heidelberg, pp. 217–247.

Bailey, W.J., Römer, H., 1991. Sexual differences in auditory sensitivity: mismatch of hearing threshold and call frequency in a tettigoniid (orthoptera, tettigoniidae: Zaprochilinae). J. Comp. Physiol. 169, 349–353. https://doi.org/10.1007/BF00206999.

Bailey, W.J., Stephen, R.O., 1978. Directionality and auditory slit function: a theory of hearing in bushcrickets. Science 80 (201), 633–634. https://doi.org/10.1126/science.201.4356.633.

Baker, A.A., Jonsson, T., Aldridge, S., Montealegre-Z, F., 2019. Complex wing motion during stridulation in the katydid *Nastonotus foreli* (Orthoptera: tettigoniidae: Pseudophyllinae). J. Insect Physiol. 114, 100–108. https://doi.org/10.1016/j.jinsphys.2019.03.005.

Beier, M., 1962. Tettigoniidae. Pseudophyllinae I. In: Das Tierreich. de Gruyter, Berlin, p. 468.

Beier, M., 1960. Tettigoniidae. Pseudophyllinae II. In: Das Tierreich. de Gruyter, Berlin, p. 396.

Belwood, J.J., 1990. Anti-predator defenses and ecology of neotropical forest katydids, especially the Pseudophyllinae. In: Bailey, W.J., Rentz, D.F.C. (Eds.), The Tettigoniidae: Biology, Systematics, and Evolution. Springer Berlin Heidelberg, pp. 8–26.

Belwood, J.J., Morris, G.K., 1987. Bat predation and its influence on calling behavior in neotropical katydids. Science 238, 64–67.

Bolívar, I., 1881. Notas entomologicas. In: An. Soc. Espan. Hist. Nat., pp. 490–491.

Celiker, E., Jonsson, T., Montealegre-Z, F., 2020. The auditory mechanics of the outer ear of the bush cricket: a numerical approach. Biophys. J. 118, 464–475. https://doi.org/10.1016/j.bpj.2019.11.3394.

Celiker, E., Woodrow, C., Rocha-sánchez, A.Y., Chivers, B.D., Barrientos-lozano, L., Montealegre-z, F., 2022. Beyond the exponential horn : a bush-cricket with ear canals which function as coupled resonators. R. Soc. Open Sci. 9.

Cigliano, M.M., Braun, H., Eades, D.C., Otte, D., 2023. Orthoptera species file version 5.0/5.0 [WWW Document]. URL. http://orthoptera.speciesfile.org. (Accessed 20 February 2023).

Geipel, I., Kernan, C.E., Litterer, A.S., Carter, G.G., Page, R.A., ter Hofstede, H.M., 2020. Predation risks of signalling and searching: bats prefer moving katydids. Biol. Lett. 16, 3–7. https://doi.org/10.1098/rsbl.2019.0837.

Hoffmann, E., Jatho, M., 1995. The acoustic trachea of Tettigoniids as an exponential horn: theoretical calculations and bioacoustical measurements. J. Acoust. Soc. Am. 98, 1845–1851. https://doi.org/10.1121/1.413371.

Jonsson, T., Montealegre-Z, F., Soulsbury, C.D., Robson Brown, K.A., Robert, D., 2016. Auditory mechanics in a bush-cricket: direct evidence of dual sound inputs in the pressure difference receiver. J. R. Soc. Interface 13, 20160560. https://doi.org/10.1098/rsif.2016.0560.

Mason, A.C., Morris, G.K., Wall, P., 1991. High ultrasonic hearing and tympanal slit function in rainforest katydids. Naturwissenschaften 78, 365–367. https://doi.org/10.1007/BF01131611.

Michelsen, A., 1979. Insect ears as mechanical systems. Am. Sci. 67, 696–706.

Michelsen, A., Larsen, O.N., 2008. Pressure difference receiving ears. Bioinspiration Biomimetics 3. https://doi.org/10.1088/1748-3182/3/1/011001.

Michelsen, A., Larsen, O.N., 1978. Biophysics of the ensiferan ear - I. Tympanal vibrations in bushcrickets (Tettigoniidae) studied with laser vibrometry. J. Comp. Physiol. 123, 193–203. https://doi.org/10.1007/BF00656872.

Montealegre-Z, F., Morris, G.K., 1999. Songs and systematics of some tettigoniidae from Colombia and Ecuador 1. Pseudophyllinae (orthoptera). J. Orthoptera Res. 8, 163–236.

Montealegre-Z, F., Morris, G.K., Mason, A.C., 2006. Generation of extreme ultrasonics in rainforest katydids. J. Exp. Biol. 209, 4923–4937. https://doi.org/10.1242/jeb.02608.

Montealegre-Z, F., Robert, D., 2015. Biomechanics of hearing in katydids. J. Comp. Physiol. 201, 5–18. https://doi.org/10.1007/s00359-014-0976-1.

Morris, G.K., Klimas, D.E., Nickle, D.A., 1989. Acoustic signals and systematics of false-leaf katydids from Ecuador (Orthoptera: tettigoniidae: Pseudophyllinae). Trans. Am. Entomol. Soc. 114, 215–263.

Morris, G.K., Mason, A.C., Wall, P., Belwood, J.J., 1994. High ultrasonic and tremulation signals in neotropical katydids (Orthoptera: tettigoniidae). J. Zool. 233, 129–163. https://doi.org/10.1111/j.1469-7998.1994.tb05266.x.

Nickle, D.A., 1992. Katydids of Panama (orthoptera: tettigoniidae). In: Quintero, D., Aiello, A. (Eds.), Insects of Panama and Mesoamerica. Selected Studies. Oxford University Press, pp. 142–184.

Nielsen, E.T., Dreisig, H., 1970. The behavior of stridulation in Orthoptera Ensifera. Behaviour 37, 205–251.

Nocke, H., 1975. Physical and physiological properties of the tettigoniid ("grasshopper") ear. J. Comp. Physiol. Sensory Neural Behav. Physiol. 100, 25–57. https://doi.org/10.1007/BF00623929.

Pulver, C.A., Celiker, E., Woodrow, C., Geipel, I., Soulsbury, C.D., Cullen, D.A., Rogers, S. M., Veitch, D., Montealegre-Z, F., 2022. Ear pinnae in a neotropical katydid (Orthoptera : tettigoniidae) function as ultrasound guides for bat detection. Elife 1–31.

Rajaraman, K., Mhatre, N., Jain, M., Postles, M., Balakrishnan, R., Robert, D., 2013. Low-pass filters and differential tympanal tuning in a paleotropical bushcricket with an unusually low frequency call. J. Exp. Biol. 216, 777–787. https://doi.org/10.1242/jeb.078352.

Reeve, R.E., Webb, B.H., 2003. New neural circuits for robot phonotaxis. Philos. Trans. R. Soc. A Math. Phys. Eng. Sci. 361, 2245–2266. https://doi.org/10.1098/rsta.2003.1274.

Rentz, D.C.F., 1979. Comments on the classification of the orthopteran family Tettigoniidae with a key to subfamilies and description of two new subfamilies. Aust. J. Zool. 27, 991–1013.

Römer, H., Holderied, M., 2020. Decision making in the face of a deadly predator: high-amplitude behavioural thresholds can be adaptive for rainforest crickets under high background noise levels: decision rule in cricket bat avoidance. Philos. Trans. R. Soc. B Biol. Sci. 375 https://doi.org/10.1098/rstb.2019.0471.

Schneider, E.S., Römer, H., Robillard, T., Schmidt, A.K.D., 2017. Hearing with exceptionally thin tympana: ear morphology and tympanal membrane vibrations in eneopterine crickets. Sci. Rep. 7, 1–12. https://doi.org/10.1038/s41598-017-15282-z.

Schulze, W., Schul, J., 2001. Ultrasound avoidance behaviour in the bushcricket *Tettigonia viridissima* (Orthoptera: tettigoniidae). J. Exp. Biol. 204, 733–740.

Song, H., Amédégnato, C., Cigliano, M.M., Desutter-Grandcolas, L., Heads, S.W., Huang, Y., Otte, D., Whiting, M.F., 2015. 300 million years of diversification: elucidating the patterns of orthopteran evolution based on comprehensive taxon and gene sampling. Cladistics 31, 621–651. https://doi.org/10.1111/cla.12116.

Stumpner, A., Dann, A., Schink, M., Gubert, S., Hugel, S., 2013. True katydids (Pseudophyllinae) from Guadeloupe: acoustic signals and functional considerations of song production. J. Insect Sci. 13, 1–16. https://doi.org/10.1673/031.013.15701.

Stumpner, A., Heller, K., 1992. Morphological and physiological differences of the auditory system in three related bushcrickets (Orthoptera: phaneropteridae, Poecilimon). Physiol. Entomol. 17, 73–80. https://doi.org/10.1111/j.1365-3032.1992.tb00992.x.

Suga, N., 1966. Ultrasonic production and its reception in some neotropical Tettigoniidae. J. Insect Physiol. 12 https://doi.org/10.1016/0022-1910(66)90119-3.

ter Hofstede, H., Voigt-Heucke, S., Lang, A., Römer, H., Page, R., Faure, P., Dechmann, D., 2017. Revisiting adaptations of neotropical katydids (Orthoptera: tettigoniidae) to gleaning bat predation. Neotrop. Biodivers. 3, 41–49. https://doi.org/10.1080/23766808.2016.1272314.

ter Hofstede, H.M., Symes, L.B., Martinson, S.J., Robillard, T., Faure, P., Madhusudhana, S., Page, R.A., 2020. Calling songs of neotropical katydids (orthoptera: tettigoniidae) from Panama. J. Orthoptera Res. 29, 137–201. https://doi.org/10.3897/JOR.29.46371.

Zou, W., Liang, H., Wu, P., Luo, B., Zhou, D., Liu, W., Wu, J., Fang, L., Lei, Y., Feng, J., 2022. Correlated evolution of wing morphology and echolocation calls in bats. Front. Ecol. Evol. 10, 1031548 https://doi.org/10.3389/fevo.2022.1031548, 1–11.